Microfluidic Janus fibers with dual thermoresponsive behavior for thermoactuation

Wasif Razzaq, Christophe A Serra, Delphine Chan-Seng

Microfluidic Janus fibers with dual thermoresponsive behavior for thermoactuation

Wasif Razzaq,[a,b] Christophe A. Serra,[a] Delphine Chan-Seng[a,*]

[a] *Université de Strasbourg, CNRS, Institut Charles Sadron UPR 22, F-67000 Strasbourg, France*
* corresponding author: delphine.chan-seng@ics-cnrs.unistra.fr

[b] *Department of Materials, National Textile University, Sheikhupura Road, Faisalabad, 37610, Pakistan*

ABSTRACT

Thermoresponsive bilayer hydrogels have gained attention due to their fast response time and excellent recovery. A side-by-side capillary-based microfluidic device has been used to produce thermoresponsive Janus fibers by photopolymerization of monomer streams. These fibers had one of their parts consisting in a thermoresponsive polymer obtained from oligo(ethylene glycol) acrylate, 2-ethoxyethyl acrylate, and poly(ethylene glycol) diacrylate, while the other one consisted in a non-thermoresponsive polymer. The fibers showed reversible coiling and uncoiling phenomena with two temperature transitions upon heating (and cooling). The unexpected dual thermoresponsiveness was investigated by screening a wide range of parameters including the nature of the photoinitiator and comonomers. The transition temperatures were tuned from 0 to 80 °C by varying the comonomer composition, but also the nature and concentration of the crosslinker used. The ability of these Janus fibers to act as thermally-triggered actuators was demonstrated by performing up to four heating-cooling cycles and attaching a small weight at one of the extremities of the fiber. These results pave the way to the development of easily tunable polymer-based fibrous thermoactuators.

KEYWORDS: Thermoresponsive fiber, Janus fiber, microfluidic spinning, actuation

1. INTRODUCTION

Polymer-based actuators are smart materials generating a motion in response to external stimuli with promising and attractive applications such as artificial muscles,[1] sensors,[2] drug release,[3] and soft robotics.[4] Hydrogels are three-dimensional networks of hydrophilic polymers able to hold a large amount of water in their swollen state. Stimuli-responsive hydrogel are gaining increasing interest in the actuating field[5] due to their ability to reversibly and significantly modify their shape and volume in response to changes occurring in their environment. A wide range of stimuli have been investigated including pH,[6, 7] temperature,[8] humidity,[9] light,[10] electric and magnetic fields,[11, 12] and ionic strength.[13] Thermoresponsive polymers have attracted the attention due to their ease of applicability, monitoring, and controllability.[14] The two main types of thermoresponsive polymers exhibit either a lower or upper critical solution temperature (LCST[15, 16] and UCST[17, 18] respectively) corresponding to the critical temperature below or above which the polymer is fully miscible in the solvent. This behavior is driven by different types of interactions such as hydrogen bonding, hydrophobic, and electrostatic interactions.[19] Among the polymers exhibiting a LCST-type behavior, poly(*N*-isopropyl acrylamide)[20] (poly(NIPAAm)) and poly(oligo(ethylene glycol acrylate)[21] (poly(OEGA)) are the most extensively investigated due to their transition temperature close to the body temperature and their non-cytotoxicity making them attractive for biomedical applications. Hydrogels made of polymers with a LCST-type phase transition, also known as gels with a negative volume phase transition (VPT) behavior shrink above the volume phase transition temperature (VPTT) and swell below the VPTT.

Conventional hydrogels, based on isotropic and homogenous materials, usually display a slow response through coiling, bending, or twisting to the applied stimulus. Anisotropic and heterogeneous structures have been developed targeting hydrogels with controllable and fast actuation. Hydrogel actuators based on either chemical or physical multilayered structures with an asymmetric response have been identified as an effective strategy to achieve sensible, fast, and tunable actuation for various stimuli including pH[22] and temperature. Bilayer hydrogel systems with thermoresponsive and fast actuation have been prepared through various methods. The most common method involves sequential layered polymerization with one of the layers generally consisting in poly(NIPAAm).[23-27] For example, Li *et al.* photopolymerized first *N*-acryloyl glycinamide followed by the photopolymerization of a mixture of *N*-isopropyl acrylamide (NIPAAm) containing Laponite used notably to improve the interface between the layers using a crosslinker in each polymerization step.[26] As the polymer layers exhibited opposite thermoresponsive behaviors (gels negative and positive VPT behavior respectively) at distinctive temperature, the cooperative contraction and expansion of each layer led to bidirectional actuation.

Layer enrichment is another method considered. He *et al.* have conducted an *in situ* polymerization-centrifugation of NIPAAm in the presence of graphene oxide leading to the formation of a graphene oxide-rich layer,[28] while Xiao *et al.* have exploited the *in situ* phase separation of poly(NIPAAm) and poly(3-(1-(4-vinylbenzyl)-1*H*-imidazol-3-ium-3-yl)propane-1-sulfonate) during their one-pot polymerization.[13] Only few examples in the literature focus on thermoresponsive bilayer fibrous structures. Li *et al.* have used electrospinning to produce fibrous bilayer system by sequential spinning of polymer solution of thermoplastic polyurethane and crosslinkable poly(NIPAAm),[29] while Meiling *et al.* have reported bilayer fibers by co-flowing aqueous solutions of sodium alginate of which one contained poly(NIPAAm) and graphene oxide in the presence of an outer aqueous fluid of calcium chloride.[30]

Herein, we report the microfluidic preparation of actuators based on tunable thermoresponsive Janus fibers. Microfluidic spinning using a side-by-side capillary-based device offers the possibility to control various features of the fibers including their diameter,[31] their morphology (Janus and Hecate),[32] but also the composition of the fibers as they can be produced from pre-existing polymers or by photopolymerization of monomers during the fiber process. These Janus fibers were produced to afford fibers with one part being thermoresponsive starting from a monomer known to form polymers exhibiting a LCST-type behavior, and the second one non-thermoresponsive as depicted in **Fig. 1**. The reversible thermoresponsive behavior was investigated to determine the effect of the (co)monomers used (**Fig. 2**) in each part of the Janus fiber and their potential as thermoactuators.

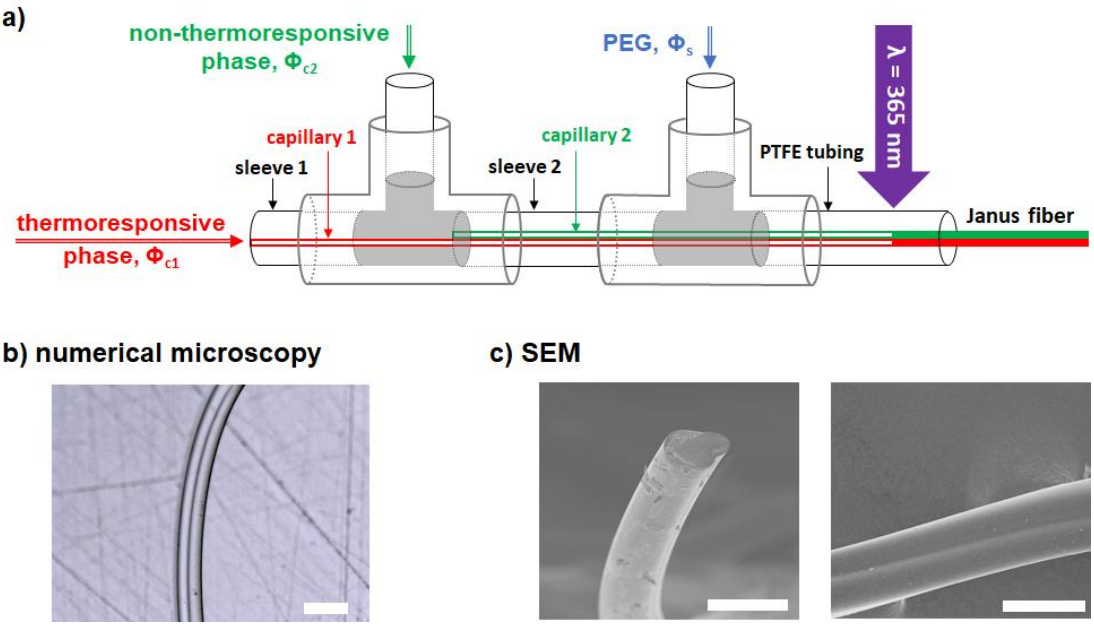

Fig. 1. Production of thermoresponsive Janus fibers: a) schematics of the side-by-side capillary-based microfluidic device, and images of the fibers by b) numerical and c) scanning electron microscopies. Scale bars = 100 µm.

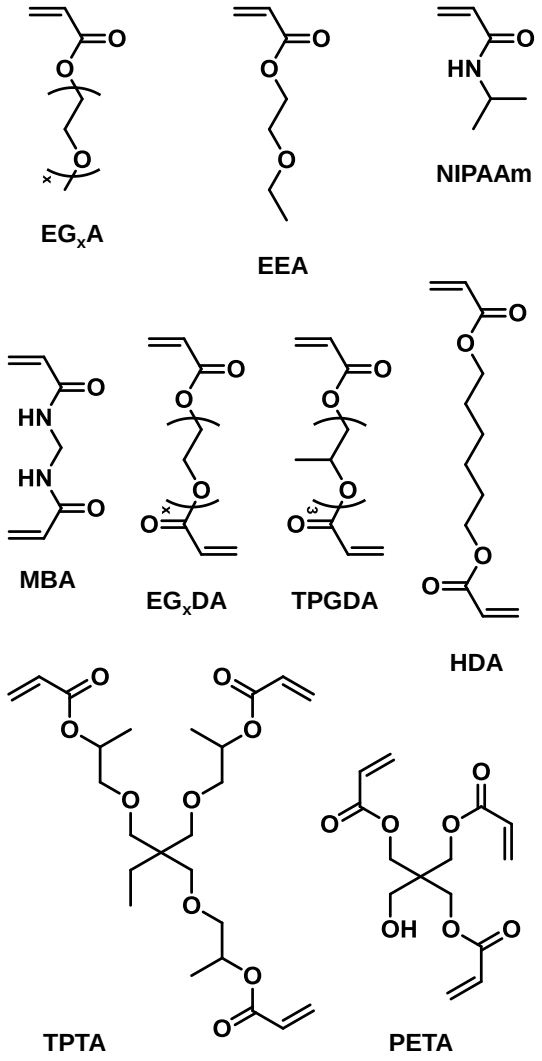

Fig. 2. Structure of the monomers used in this work.

2. RESULTS AND DISCUSSION

2.1. Preparation of Janus fibers comprising one thermoresponsive phase (EG_3A/EEA/EG_6DA 50/50/2)

The thermoresponsive Janus fibers were prepared using a side-by-side capillary-based microfluidic system[32] with three phases: i) a first core phase that will produce the thermoresponsive part of the Janus fiber (Φ_{c1}), ii) a second core phase leading to the non-thermoresponsive one (Φ_{c2}), and iii) the sheath phase (Φ_s). Φ_{c1} was a ternary monomer system, composed of tri(ethylene glycol) acrylate (EG_3A), 2-ethoxyethyl acrylate (EEA), and poly(ethylene glycol) diacrylate with a number-average molecular weight of 400 g·mol^{-1} (EG_6DA) to promote crosslinking, in the presence of Irgacure 369 (3 w/v%) used as

photoinitiator in ethanol (20 v% relative to EG_3A and EEA). Φ_{c2} consisted of EG_6DA (60 v/v%) in the presence of Irgacure 369 (3 w/v%) in ethanol (40 v/v%), while Φ_s was poly(ethylene glycol) with a number-average molecular weight of 300 $g \cdot mol^{-1}$ (PEG 300). The molar ratio in comonomers in Φ_{c1} was fixed to 50/50 for EG_3A /EEA in the presence of 2 mol% of EG_6DA. Φ_{c1} and Φ_{c2} were polymerized upon UV irradiations at 365 nm in the microfluidic system under flow. The fiber had an average diameter of 60 µm as determined by numerical microscopy and were homogeneous all along the fiber.

The reversible thermoresponsive behavior was observed by immersing one fiber hold at one of its extremities in a thermoregulated water bath (**Fig. 3**). The fiber was fully extended around 18 °C, while the fiber started coiling below 16 °C and above 20 °C. The coiling phenomenon became more pronounced by further decreasing or increasing the temperature respectively from their transition temperatures. According to the literature, poly(EG_3A) exhibits a clearing point upon heating ($T_{CL,h}$) at 70 °C,[21] which could not be compared to the Janus fibers prepared without using EEA. Indeed, it was impossible to work with this open water bath system at the elevated temperature required for this measurement due the high Brownian motion observed.

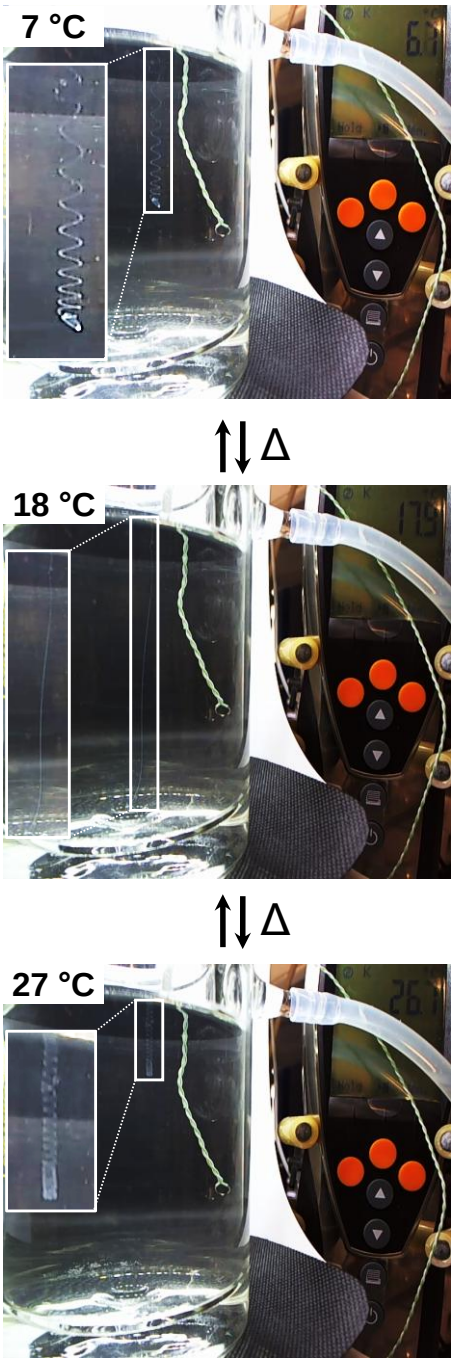

Fig. 3. Images illustrating the coiling and uncoiling phenomena of thermoresponsive Janus fibers (thermoresponsive part: EG_3A/EEA 50/50 with 2 mol% of EG_6DA, non-thermoresponsive part: EG_6DA) upon heating and cooling cycles. The setup consisted in a water-filled jacked vessel connected to a circulating thermoregulated bath with a thermocouple immersed for temperature recording. The corresponding video is available as supplementary material (the speed of the video was accelerated by 30x).

2.2. Identification of the parameters responsible of the dual behavior observed

Poly(oligo ethylene glycol acrylate)s have been widely investigated for their LCST-type behavior in aqueous solution and UCST-type behavior in alcoholic solution.[21, 33] The Janus fibers prepared

without using EG_3A did not show any thermoresponsive behavior confirming that this behavior was attributed to EG_3A. However, the low value of the transition temperature observed was imputed to the presence of EEA repeat units as suggested by the work of Mueller showing a decrease of the transition temperature of poly(*N*,*N*-dimethyl acrylamide) with the increase of the content in EEA.[34]

However, the UCST-type behavior of PEG-based homopolymers in pure water is rarely reported. Saeki *et al.* have investigated the phase separation behavior of PEG in water under saturated vapor pressure exhibiting a loop-type diagram with LCST and UCST as low as 99 and 216 °C respectively. These values depended on the molecular weight of the PEG used, while the gap between the LCST and UCST was narrower when decreasing the molecular weight of the PEG chains.[35] Hammouda *et al.* have demonstrated an UCST-type behavior of PEG above the boiling point of water by small-angle neutron scattering under pressurized conditions.[36] The groups of Wu[37] and Tam[38] have reported an aggregation process induced by the temperature for oligo(ethylene glycol) methacrylate copolymers involving in the formation of loose aggregates followed by a reorganization of the polymer chains leading to more densely packed aggregates. Usually, UCST and LCST-type behaviors are observed by copolymerization of PEG-based monomers with monomers known to exhibit an UCST-type behavior especially in alcoholic solutions.[39-41] Control experiments were thus conducted to identify the source of this dual thermoresponsive behavior. The contribution of the Janus morphology of the fiber on the thermoresponsive behavior was investigated by preparing fibers composed solely of the thermoresponsive part using a similar microfluidic system with solely two phases (Φ_{c1} and Φ_s). The thermoresponsive behavior was observed, but was less noticeable especially the positive VPT response as compared to the Janus one. This suggests that the presence of the non-thermoresponsive part of the Janus may restrict the free rearrangement of the polymer chains in the thermoresponsive part during the transition. It is likely due to the interface with the non-thermoresponsive part of the fiber which induced a more pronounced bending of the fiber.

To discriminate between the nature of the polymer and the potential role of the fiber morphology, polymer hydrogel strips were prepared by photopolymerization of EG_3A, EEA, and EG_6DA in the presence of Irgacure 369 in ethanol by solution casting on a horizontal balanced surface under UV irradiations at 365 nm. The thermoresponsive behavior of this hydrogel in water was investigated by turbidimetry at 540 nm by placing a polymer strip (250 mg) in pure water (2 mL) and conducting a heating and cooling cycle between 8 and 50 °C using a temperature ramp of 1 °C·min^{-1}. The polymer exhibited both negative and positive VPT behaviors and the cloud (T_{CP}) and clearing (T_{CL}) points (“h” and “c” indicates if the transition temperature is recorded upon heating or cooling respectively) were

determined at the inflexion point[42] on the heating and cooling curves as $T_{CP,h}$ = 21 °C, $T_{CL,h}$ = 19 °C, $T_{CP,c}$ = 16 °C, and $T_{CL,c}$ = 19 °C (**Fig. 4**). The values were close to those determined for the Janus fiber.

Furthermore, Janus fibers prepared using NIPAAm and EG_6DA in the feed of the thermoresponsive part exhibited also the dual thermoresponsive behavior (**Fig. S1**) indicating that this dual thermoresponsive phenomenon was not specific to polymers based on EG_3 and EEA in the presence of EG_6DA. Overall, these results indicated that the dual behavior was not related to the fiber nature and monomer composition in the thermoresponsive part of the fiber.

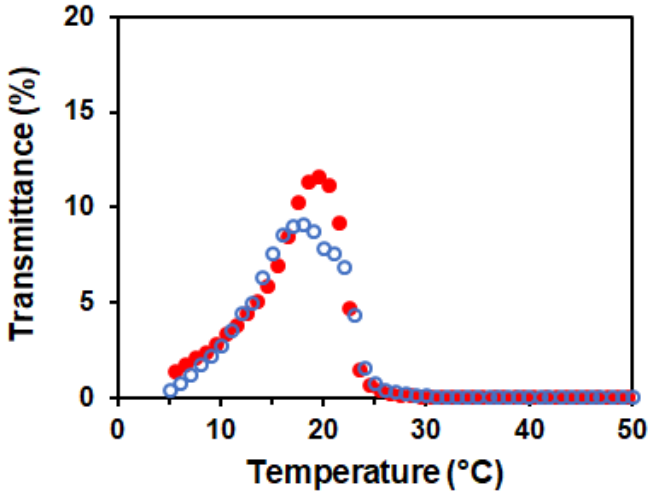

Fig. 4. Turbidity curves for polymer strips prepared from EG_3A/EEA (50/50 mol%) with 2 mol% of EG_6DA in water upon heating (●) and cooling (○).

Hydrogel strips were produced using four different photoinitiators (**Fig. 5a**) and turbidity measurements (**Fig. 5b**) were performed on them (the differences in transmission intensity and shape observed were mainly due to the inconsistencies in thickness of the hydrogel and the shape of the hydrogel (strip) leading to heterogeneity of the sample in the cuvette and thus in the spectroscopy measurement). Two trends were noticeable: the hydrogels obtained from photoinitiators having a morpholino group exhibited the dual thermoresponsive behavior, while the other ones showed only the expected negative VPT behavior. These results seemed to suggest that the morpholino groups may be potentially involved in some self-assembly mechanisms leading to the uncoiling transition observed at low temperature upon heating.

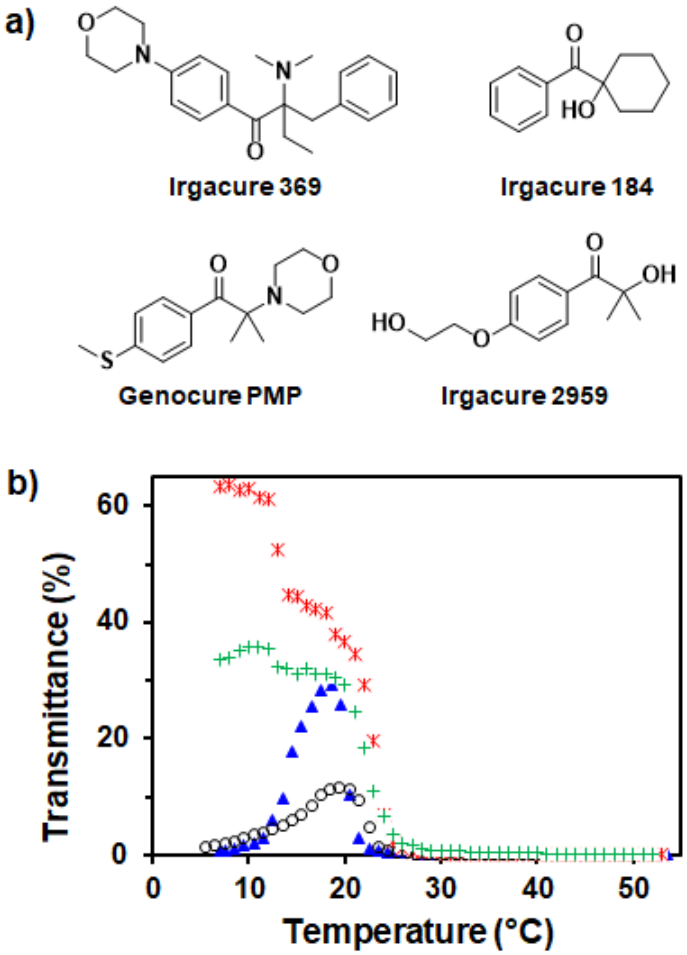

Fig. 5. Effect of the initiator used on the thermal behavior of poly(EGDA) hydrogels prepared from EG_3A/EEA (50/50 mol%) : a) Structure of the photoinitiators used and b) turbidity curves upon heating/cooling for Irgacure 369 (○), Genocure PMP (▲), Irgacure 184 (+), and Irgacure 2959 (✳).

EG_3A and EEA were also photopolymerized without the crosslinker EG_6DA. The polymer dissolved in water at a concentration of 5 µL·mL^{-1} was characterized similarly by turbidimetry. Solely the LCST-type behavior was observed (**Fig. 6**). The presence of the positive VPT behavior in water for the crosslinked fiber could be driven by the crosslinked points. Another possibility could be that the non-crosslinked polymer had an UCST-type behavior out of the temperature range considered here. Xia *et al.* have previously reported hydrogels based on poly(oligo(ethylene glycol) methacrylate-*co*-2-(2-methoxyethoxy)ethyl methacrylate) in the presence of clay acting as physical crosslinker displaying both negative and positive VPT behaviors.[43] However, when the clay was replaced by MBA as covalent crosslinker the authors solely observed the negative VPT behavior. For our system, when EG_6DA was replaced by MBA both transition temperature leading to coiling (T_C) or uncoiling (T_U) were still observed with $T_{U,h}$ = 35 °C and $T_{C,h}$ = 36 °C upon heating ($T_{U,c}$ = 34 °C and $T_{C,c}$ = 33 °C upon cooling) for the polymer

strips obtained. Altogether, we presume that this unexpected dual behavior could be attributed to the structure of the photoinitiator inducing the phase transition behavior observed at low temperature by self-assembly that was enhanced through hindrance imposed by the non-thermoresponsive part of the Janus fibers and the crosslinking points in its thermoresponsive part.

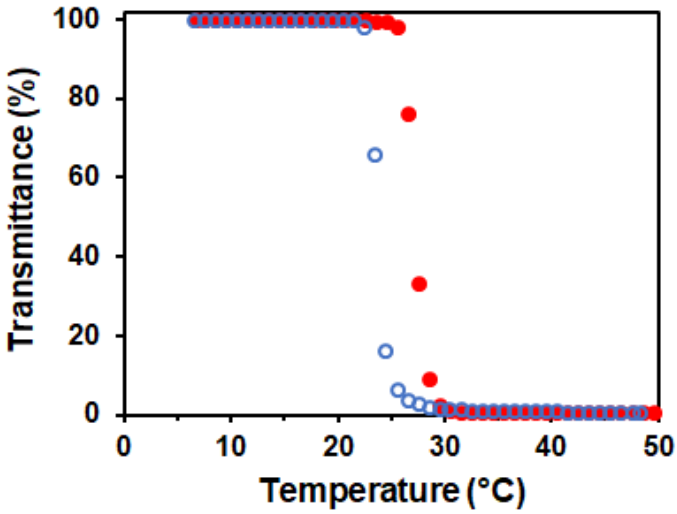

Fig. 6. Turbidity curves for polymer solutions prepared from EG_3A/EEA (50/50 mol%) without crosslinker (EG_6DA) in water upon heating (●) and cooling (○).

2.3. Effect of the comonomers in the feed forming the thermoresponsive part of the Janus fibers

The comonomer ratio EG_3A/EEA was varied from 30/70 to 70/30 while maintaining all other parameters constant and identical to the previous experiments. Upon heating and cooling, the uncoiling and coiling points were recorded and plotted against the content in EG_3A used in the EG_3A/EEA comonomer feed (**Fig. S2a**). The temperature of both transitions increased with the content in EG_3A ranging from 12 to 30 °C for the coiling transition upon heating. No significant difference was observed for the value of the transition temperatures upon heating and cooling, while the uncoiling and coiling transitions were almost systematically having a miscibility gap of 3-4 °C. To widen the range of thermoresponsive Janus fibers accessible through this approach and thus adapt to the requirement of the targeted applications, EG_3A was replaced by poly(ethylene glycol) methyl ether acrylate (EG_9A) in the comonomer feed. By varying the EG_9A/EEA comonomer feed from 10/90 to 30/70, the same tendency was observed with transition temperature ranging from 18 to 50 °C for the VPT upon heating (**Fig. S2b**). The changes observed for the transition temperatures were caused by the hydrophilic/hydrophobic contributions of the comonomers in the copolymer,[43, 44] where EEA provided more hydrophobicity and oligo(ethylene glycol) acrylates more hydrophilicity.[21] The increase in EG_9A or EG_3A contents in the copolymer led

thus to higher transition temperatures due to the increased hydrophilic nature of the copolymer and a linear correlation between the transition temperature observed and the content in ethylene glycol units from EG_9A or EG_3A (**Fig. 7**).

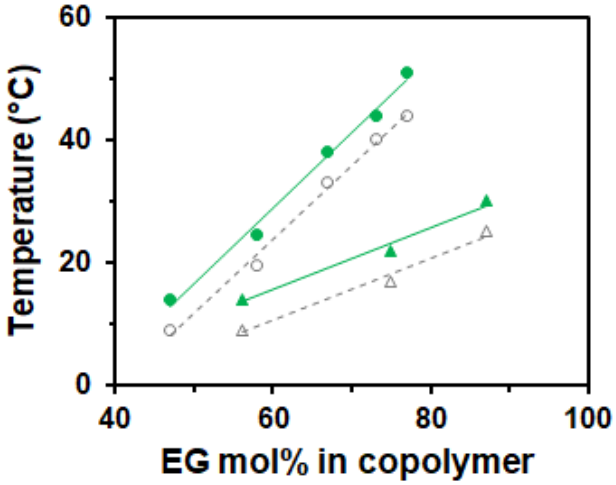

Fig. 7. Effect of the content in ethylene glycol (EG) in the copolymer constituting the thermoresponsive part of Janus fibers on the transition temperature upon heating for the systems EEA/EG_9A (circles) and EEA/EG_3A (triangles). The filled green symbols correspond to the uncoiling points ($T_{U,h}$) and the open grey symbols to the coiling transition ($T_{C,h}$).

2.4. Effect of the crosslinker used in the thermoresponsive part of the Janus fiber

The effect of crosslinker concentration was investigated by varying EG_6DA from 0 to 16 mol% relative to EG_3A that was used as sole monomer in the feed of the thermoresponsive part of the Janus fibers. The values of transition temperatures decreased linearly with the increased content in crosslinker (**Fig. 8**) that could be attributed to the lower swelling capacity of the hydrogel. The same trend was observed when replacing EG_6DA by EG_3DA and crosslinker concentration between 0 and 30 mol% with a steeper slope attributed to its lower hydrophilicity as reported previously.[45] The hydrophilicity/hydrophobicity nature of the crosslinker was further studied by selecting diacrylate with various numbers of ethylene glycol units ($EG_{10}DA$, EG_9DA, EG_3DA, and EG_2DA), but also diacrylate bearing hydrophobic units such as tri(propylene glycol) diacrylate (TPGDA) and 1,6-hexanediol diacrylate (HDA).[46] The higher the number of ethylene glycol units per diacrylate crosslinker (and thus the hydrophilicity), the higher the values of the transition temperatures (**Table 1**). This statement was consistent with the trend observed for the comonomers used in the feed. The use of hydrophobic diacrylate crosslinkers (TPGDA and HDA) led to even lower transition temperatures with a larger miscibility gap of 10 °C as compared to what was observed previously (3-4 °C).

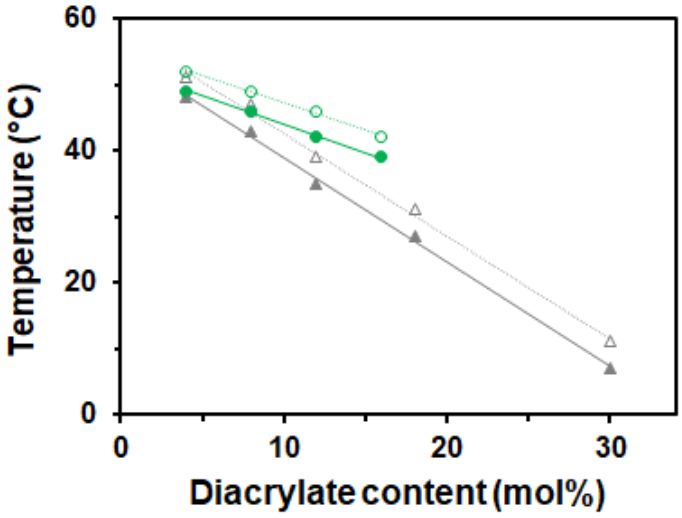

Fig. 8. Effect of the crosslinker (EG_6DA, green circles or EG_3DA, grey triangle) concentration on the uncoiling (filled symbols) and coiling (open symbols) transition temperature.

Table 1. Effect of the nature of the diacrylate crosslinker on the transition temperatures (thermoresponsive part: 88/12 EG_3A/diacrylate crosslinker; non-thermoresponsive part: EG_6DA)

diacrylate crosslinker	$T_{U,h}$ (°C)	$T_{C,h}$ (°C)	$T_{U,c}$ (°C)	$T_{C,c}$ (°C)
$EG_{10}DA$	48	52	51	47
EG_9DA	42	48	47	40
EG_3DA	37	39	39	36
EG_2DA	37	41	40	35
TPGDA	11	21	16	6
HDA	7	17	17	6

Crosslinkers with three acrylate groups, *i.e.* pentaerythritol triacrylate (PETA) and trimethylolpropane propoxylate triacrylate with a number-average molecular weight of 644 $g \cdot mol^{-1}$ (TPTA), were substituted to the diacrylate crosslinker to evaluate the influence of the functionality of the crosslinker on the transition temperatures (**Table 2**). PETA was investigated using the same concentration in crosslinker (12 mol% in triacrylate) and in acrylate groups (8 mol% in triacrylate), while these concentrations could not be used for TPTA as the transition temperatures were not measurable since below water freezing point leading to the production of fibers with lower concentration in triacrylates (2 and 4 mol%). Considering TPGDA and TPTA being the respective diacrylate and triacrylate crosslinkers having the closest chemical structure, the data indicated that the higher functionality of TPTA led to a shift of the transition temperature of lower values due to the more densely crosslinked network. The increase in crosslinker concentration led to a significant decrease in the value of the transition temperatures for TPTA as

expected, but surprisingly for PETA the inverse tendency was observed. The miscibility gap for the triacrylates was slightly higher (15 °C on average) than the one observed when using the hydrophobic diacrylate (TPGDA and HDA).

Table 2. Triacrylate crosslinkers and their effects on the transition temperatures upon heating and cooling (thermoresponsive part: EG_3A/triacrylate crosslinker; non-thermoresponsive part: EG_6DA)

Triacrylate crosslinker (Content in feed, mol%)	$T_{U,h}$ (°C)	$T_{C,h}$ (°C)	$T_{U,c}$ (°C)	$T_{C,c}$ (°C)
PETA (12)	62	- [a]	- [a]	58
PETA (8)	39	52	50	37
TPTA (4)	- [b]	11	5	- [b]
TPTA (2)	33	49	44	28

[a] not determined as expected to be above 78 °C, temperature at which Brownian motion was too intense and the fiber was not properly suspended in water; [b] not determined as expected to be below 0 °C (water freezing point)

2.5. Effect of the non-thermoresponsive part of the Janus fiber

Fibers were prepared solely from EG_6DA, but also NOA89 (a photocurable prepolymer) and triethylene glycol diacrylate (TPGDA), to confirm their non-thermoresponsiveness (**Fig. S3**). Janus fibers were then produced by changing the nature of the non-thermoresponsive part of the Janus fibers considering TPGDA and NOA89 while the thermoresponsive part was obtained from 70/30 EG_3A/EEA. The uncoiling-coiling phenomenon was observed in all cases investigated here without significant impact of the nature of the non-thermoresponsive part of the Janus fibers on the transition temperature (**Fig. 9)**. This feature should provide flexibility to design the Janus fibers according to the needs by controlling the thermoresponsive behavior through the composition of one part of the Janus fiber and the mechanical properties through the other one as previously demonstrated.[32]

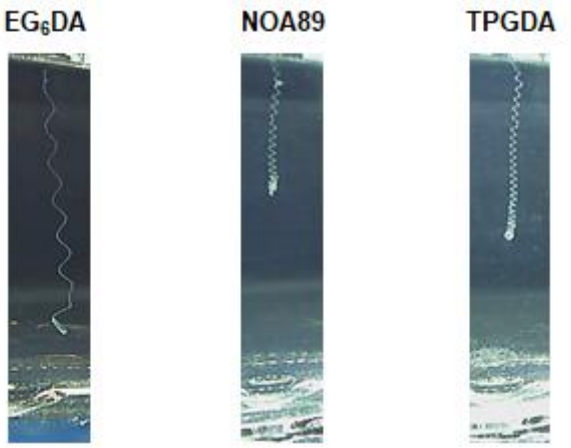

Monomer feed	$T_{U,h}$ (°C)	$T_{C,h}$ (°C)	$T_{U,c}$ (°C)	$T_{C,c}$ (°C)
EG_6DA	25	30	29	25
TPGDA	26	31	30	26
NOA89	25	30	29	24

Fig. 9. Coiling behavior of Janus fibers produced with different non-thermoresponsive feeds (thermoresponsive part prepared with 70/30 EG_3A/EEA) and their transition temperatures upon heating and cooling reported in the embedded table. The pictures were taken when the water bath was thermostated at 48 °C (when the fibers have reached the most compact coiled stage).

2.6. Thermoactuation

The potential of these Janus fibers as thermally-triggered actuators was first evaluated by performing four heating-cooling cycles on a single Janus fiber of 25/75 EG_9A/EEA (**Fig. 10a**). For each cycle, well-defined coiling and uncoiling of the fiber was observed with minimal changes in the values of the transition temperatures revealing the repeatability of their actuation. The slight differences were attributed to the difficulty to determine exactly the temperature at which the coiling/uncoiling phenomenon starts. The actuation ability of the thermoresponsive Janus fibers was further demonstrated by suspending a weight of 30 mg on a single fiber in the thermoregulated water bath heated from 15 to 60 °C and taking pictures of the setup below $T_{U,h}$ (17 °C), between $T_{U,h}$ and $T_{C,h}$ (35 °C), and above $T_{C,h}$ (58 °C). The uncoiling transition (from 17 to 35 °C) led to an extension of the fiber of 0.5 cm, while the coiling transition (from 35 to 58 °C) showed a contraction of 2.5 cm (**Fig. 10b**).

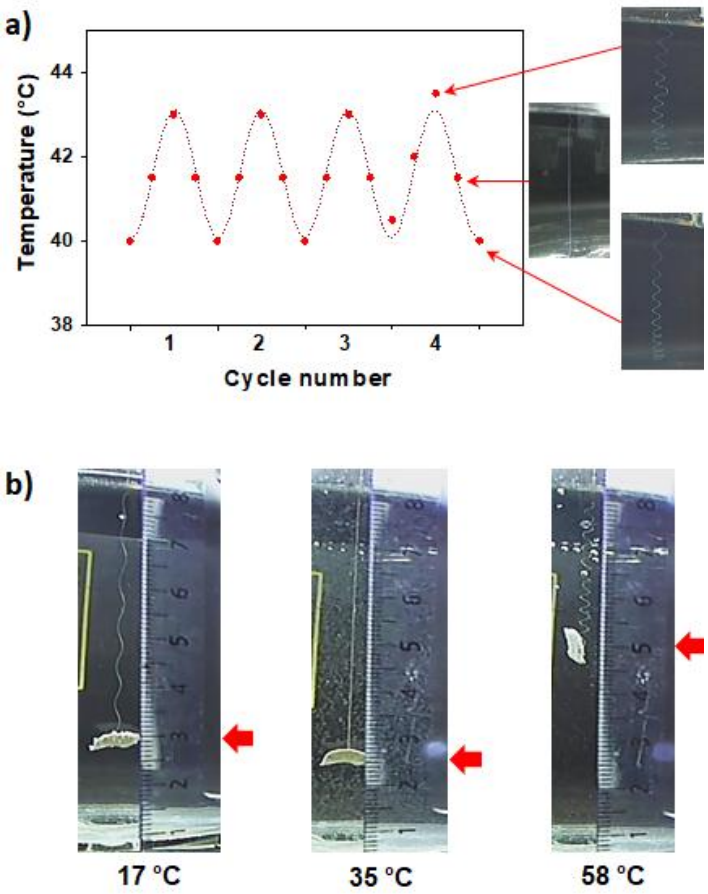

Fig. 10. Thermoactuation of the Janus fibers: (a) repeatability over four heating-cooling cycles (thermoresponsive part: 25/75 EG_9A/EEA with 2 mol% of EG_6DA; non-thermoresponsive part: EG_6DA) and (b) displacement of a small weight upon heating (thermoresponsive part: 20/80 EG_9A/EEA with 2 mol% of EG_6DA; non-thermoresponsive part: EG_6DA).

3. CONCLUSION

In summary, thermoresponsive Janus hydrogel fibers were successfully prepared by photopolymerization of monomers using a side-by-side capillary-based microfluidic device. These fibers exhibited coiling and uncoiling phenomena upon heating and cooling with two temperature transitions that could be tuned thanks to the composition of the thermoresponsive part of the Janus fibers. The coiling phenomenon upon heating was due to the nature of the thermoresponsive polymer exhibiting a negative VPT behavior, while the uncoiling could be attributed to the nature of the photoinitiator that could lead to some self-assembly driven by the morpholino groups at lower temperature. The coiling and uncoiling phenomena were emphasized by restrictions due to the nature of the crosslinker used and the non-thermoresponsive part of the Janus fibers, while offering the access to materials with different

mechanical properties. The preliminary evaluation of these fibers as thermoactuators is very promising and pave the way to the development of easily tunable polymer-based fibrous thermoactuators.

4. EXPERIMENTAL

4.1. Materials

Poly(ethylene glycol) methyl ether acrylate with a number-average molecular weight of 480 g.mol^{-1} (EG_9A, Sigma Aldrich), methoxy triethylene glycol methyl ether acrylate (EG_3A, >95.0%, TCI), 2-ethoxyethyl acrylate (EEA, 98.0%, Sigma Aldrich), tri(propylene glycol) diacrylate (TPGDA, Sartomer SR 306), poly(ethylene glycol) diacrylate with a number-average molecular weight of 575 g·mol^{-1} ($EG_{10}DA$, Sigma Aldrich), poly(ethylene glycol) diacrylate with a number-average molecular weight of 400 g·mol^{-1} (EG_6DA, Polysciences), poly(ethylene glycol) diacrylate with a number-average molecular weight of 250 g·mol^{-1} (EG_3DA, Sigma Aldrich), di(ethylene glycol) diacrylate (EG_2DA, 75%, Sigma Aldrich), *N*-isopropyl acrylamide (NIPAAm, > 98%, stabilized with MEHQ, TCI), 1,6-hexanediol diacrylate (HDA, 99.0%, Alfa Aesar), pentaerythritol triacrylate (PETA, Sigma Aldrich), trimethylolpropane propoxylate triacrylate (TPTA, M_n = 644 g·mol^{-1}, Sigma Aldrich), NOA 89 (photopolymerizable precursor, Norland), ethanol (99.9%, Carlo Erba), Irgacure 369 (Ciba), Irgacure 2959 (TCI), Irgacure184 (Ciba), Genocure PMP (Rahn AG), PEG 300 (Sigma Aldrich) were used as received.

4.2. Characterizations

Microscopy. The overall diameter of the microfibers was measured using a numerical microscope (Keyence, VHX-J100T) with variable resolution ranging from 100 to 1000x. Scanning electron microscopy (SEM) images were obtained on a Hitachi SU 8010 Ultra High-Resolution FE-SEM microscope at 1.0 kV. The fibers placed on the sample holder were held with carbon tape (Agar Scientific).

Thermoresponsive behavior. The thermoresponsive behavior was visually investigated by observing the fibers, attached at one of their extremities to a fixed needle and freely suspended into a water-filled double-jacket glass vessel connected to a circulating thermoregulated bath (**Fig. S1**). The change of conformation of the fiber upon heating and cooling between 8 and 55 °C, exhibiting coiling and uncoiling according to the temperature of the water bath was captured using a webcam. The coiling (T_C) and uncoiling (T_U) points were carefully estimated using a thermocouple immersed in the water bath by recording the transition when it starts to change from coiled to straight or straight to coiled respectively (h and c will be added in subscript to T_C and T_U if the phenomenon is observed during the heating and cooling step respectively).

UV-VIS spectrophotometry. The turbidity experiments were conducted on a UV-visible-NIR Varian Cary 5000 spectrophotometer equipped with temperature controller (±0.1 °C) at 550 nm using a heating and cooling rate of 1 °C·min^{-1}.

4.3. Preparation of thermoresponsive Janus fibers

The side-by-side capillary-based microfluidic system previously reported[31] was used to prepare the thermoresponsive Janus fibers. Thermoresponsive Janus fibers, in which one part consisted of thermoresponsive polymer and the other one of non-thermoresponsive polymer, were produced using two core phases and one sheath phase (Φ_{sheath}). Core phase 1 (Φ_{c1}, thermoresponsive phase) consisted of EG_9A, EEA, EG_6DA, and Irgacure 369 in ethanol. Core phase 2 (Φ_{c2}, non-thermoresponsive phase) was composed of EG_6DA (60 v/v%) and Irgacure 369 (3 w/v%) in ethanol (40 v/v%). The core phases were injected at specific flow rates at the first T-junction thanks to syringes pumps (PHD 2000, Harvard Apparatus) through capillary 1 and capillary 2 (internal diameter = 50 µm, outer diameter = 150 µm) which were arranged side-by-side. Both Φ_{c1} and Φ_{c2} exited at the tip of their respective capillary and got in contact to each other as well as with the sheath phase which was introduced with a second T-junction and another syringe pump. The flow rates of Φ_{c1}, Φ_{c2}, and sheath phase was Q_{c1} = 4 µL/min, Q_{c2} = 2 µL/min, Q_{sheath} = 550 µL/min respectively. Both core phases spontaneously formed two parallel streams of monomers due to shear and elongational force imposed by the flowing sheath fluid. Further down to the capillaries' tip, the monomers streams were photo-polymerized while moving in a PTFE tubing using an UV lamp operating at a wavelength of 365 nm (Lighting cure LC 8, Hamamatsu). The polymerized microfibers were collected into a water bath, washed with water and ethanol to remove the PEG sheath phase present at the surface of the fibers, and dried under ambient air overnight to remove any traces of water and ethanol.

4.4. Control photopolymerization

The hydrogel strips were prepared by mixing EG_3A and EEA in 50/50 mol% to which EG_6DA (2 mol%) was added along with Irgacure 369 (3 w/v%). The homogenous mixture was poured on a glass slide placed on leveled surface in a closed dark box having an inlet for the probe of UV lamp. The surface was exposed to UV irradiations for the duration of time (0.6 min) as for the fiber systems. The hydrogel strips were removed from the surface and washed with water and ethanol. The strips were inserted in the quartz cuvette to perform the turbidimetry measurement.

For non-crosslinked system, the solution of EG_3A/EEA (50/50 mol%) and Irgacure 369 (3 w/v%) was prepared in a vial without adding the diacrylate crosslinkers and the vial was irradiated under UV in the dark box for the same duration of time.

DATA AVAILABILTY

The raw/processed data required to reproduce these findings cannot be shared at this time due to technical or time limitations.

CREDIT AUTHORSHIP CONTRIBUTION STATEMENT

Razzaq Wasif: conceptualization, methodology, investigation, visualization, writing; **Christophe Serra:** supervision; **Delphine Chan-Seng:** conceptualization, supervision, visualization, writing.

DECLARATION OF COMPETING INTEREST

The authors declare that they have no known competing financial interests or personal relationships that could have appeared to influence the work reported in this paper.

ACKNOWLEDGEMENTS

W. R. is thankful to the Higher Education Commission Pakistan for his Ph.D. scholarship. The authors thanks I. A. Acuña Mejía for her help in running some additional experiments. This work of the Interdisciplinary Institute HiFunMat, as part of the ITI 2021-2028 program of the University of Strasbourg, CNRS and Inserm, was supported by IdEx Unistra (ANR-10-IDEX-0002) and SFRI (STRAT'US project, ANR-20-SFRI-0012) under the framework of the French Investments for the Future Program. The authors thank the electron microscopy facilities at the Institut Charles Sadron.

REFERENCES

[1] Z. Zhao, R. Fang, Q. Rong, M. Liu, Bioinspired nanocomposite hydrogels with highly ordered structures, Adv. Mater. 29(45) (2017) 1703045.

[2] C.-Y. Lo, Y. Zhao, C. Kim, Y. Alsaid, R. Khodambashi, M. Peet, R. Fisher, H. Marvi, S. Berman, D. Aukes, X. He, Highly stretchable self-sensing actuator based on conductive photothermally-responsive hydrogel, Mater. Today 50 (2021) 35-43.

[3] Y.-Q. Wang, X.-Y. Dou, H.-F. Wang, X. Wang, D.-C. Wu, Dendrimer-based hydrogels with controlled drug delivery property for tissue adhesion, Chin. J. Polym. Sci. 39(11) (2021) 1421-1430.

[4] Y. Zhou, C. Wan, Y. Yang, H. Yang, S. Wang, Z. Dai, K. Ji, H. Jiang, X. Chen, Y. Long, Highly stretchable, elastic, and ionic conductive hydrogel for artificial soft electronics, Adv. Funct. Mater. 29(1) (2019) 1806220.

[5] L. Ionov, Hydrogel-based actuators: Possibilities and limitations, Mater. Today 17(10) (2014) 494-503.

[6] S. Dai, P. Ravi, K.C. Tam, pH-Responsive polymers: Synthesis, properties and applications, Soft Matter 4(3) (2008) 435-449.

[7] Z. Han, P. Wang, G. Mao, T. Yin, D. Zhong, B. Yiming, X. Hu, Z. Jia, G. Nian, S. Qu, W. Yang, Dual pH-responsive hydrogel actuator for lipophilic drug delivery, ACS Appl. Mater. Interfaces 12(10) (2020) 12010-12017.

[8] B. Maiti, A. Abramov, L. Franco, J. Puiggalí, H. Enshaei, C. Alemán, D.D. Díaz, Thermoresponsive shape-memory hydrogel actuators made by phototriggered click chemistry, Adv. Funct. Mater. 30(24) (2020) 2001683.

[9] M. Zheng, T.-J. Long, X.-L. Chen, J.-Q. Sun, Humidity-responsive bilayer actuators comprised of porous and nonporous poly(acrylic acid)/poly(allylamine hydrochloride) films, Chin. J. Polym. Sci. 37(1) (2019) 52-58.

[10] Y. Huang, Q. Yu, C. Su, J. Jiang, N. Chen, H. Shao, Light-responsive soft actuators: Mechanism, materials, fabrication, and applications, Actuators 10(11) (2021) 298.

[11] H. Jiang, L. Fan, S. Yan, F. Li, H. Li, J. Tang, Tough and electro-responsive hydrogel actuators with bidirectional bending behavior, Nanoscale 11(5) (2019) 2231-2237.

[12] H. Li, G. Go, S.Y. Ko, J.-O. Park, S. Park, Magnetic actuated pH-responsive hydrogel-based soft micro-robot for targeted drug delivery, Smart Mater. Struct. 25(2) (2016) 027001.

[13] S. Xiao, M. Zhang, X. He, L. Huang, Y. Zhang, B. Ren, M. Zhong, Y. Chang, J. Yang, J. Zheng, Dual salt- and thermoresponsive programmable bilayer hydrogel actuators with pseudo-interpenetrating double-network structures, ACS Appl. Mater. Interfaces 10(25) (2018) 21642-21653.

[14] N. Thakur, A. Sargur Ranganath, K. Sopiha, A. Baji, Thermoresponsive cellulose acetate-poly(*N*-isopropylacrylamide) core-shell fibers for controlled capture and release of moisture, ACS Appl. Mater. Interfaces 9(34) (2017) 29224-29233.

[15] Q. Zhang, C. Weber, U.S. Schubert, R. Hoogenboom, Thermoresponsive polymers with lower critical solution temperature: From fundamental aspects and measuring techniques to recommended turbidimetry conditions, Mater. Horiz. 4(2) (2017) 109-116.

[16] M.T. Cook, P. Haddow, S.B. Kirton, W.J. McAuley, Polymers exhibiting lower critical solution temperatures as a route to thermoreversible gelators for healthcare, Adv. Funct. Mater. 31(8) (2021) 2008123.

[17] J. Seuring, S. Agarwal, Polymers with upper critical solution temperature in aqueous solution, Macromol. Rapid Commun. 33(22) (2012) 1898-1920.

[18] J. Niskanen, H. Tenhu, How to manipulate the upper critical solution temperature (UCST)?, Polym. Chem. 8(1) (2017) 220-232.

[19] H. Zhang, J. Zhang, W. Dai, Y. Zhao, Facile synthesis of thermo-, pH-, CO_2- and oxidation-responsive poly(amido thioether)s with tunable LCST and UCST behaviors, Polym. Chem. 8(37) (2017) 5749-5760.

[20] S. Lanzalaco, E. Armelin, Poly(*N*-isopropylacrylamide) and copolymers: A review on recent progresses in biomedical applications, Gels 3(4) (2017) 36.

[21] G. Vancoillie, D. Frank, R. Hoogenboom, Thermoresponsive poly(oligo ethylene glycol acrylates), Prog. Polym. Sci. 39(6) (2014) 1074-1095.

[22] P.D. Topham, J.R. Howse, C.J. Crook, S.P. Armes, R.A.L. Jones, A.J. Ryan, Antagonistic triblock polymer gels powered by pH oscillations, Macromolecules 40(13) (2007) 4393-4395.

[23] W.J. Zheng, N. An, J.H. Yang, J. Zhou, Y.M. Chen, Tough Al-alginate/poly(N-isopropylacrylamide) hydrogel with tunable LCST for soft robotics, ACS Appl. Mater. Interfaces 7(3) (2015) 1758-1764.

[24] Y. Hu, J.S. Kahn, W. Guo, F. Huang, M. Fadeev, D. Harries, I. Willner, Reversible modulation of DNA-based hydrogel shapes by internal stress interactions, J. Am. Chem. Soc. 138(49) (2016) 16112-16119.

[25] Y. Shin, J. Choi, J.-H. Na, S.Y. Kim, Thermally triggered soft actuators based on a bilayer hydrogel synthesized by gamma ray irradiation, Polymer 212 (2021) 123163.

[26] J. Li, Q. Ma, Y. Xu, M. Yang, Q. Wu, F. Wang, P. Sun, Highly bidirectional bendable actuator engineered by LCST-UCST bilayer hydrogel with enhanced interface, ACS Appl. Mater. Interfaces 12(49) (2020) 55290-55298.

[27] Y. Cheng, C. Huang, D. Yang, K. Ren, J. Wei, Bilayer hydrogel mixed composites that respond to multiple stimuli for environmental sensing and underwater actuation, J. Mater. Chem. B 6(48) (2018) 8170-8179.

[28] X. He, Y. Sun, J. Wu, Y. Wang, F. Chen, P. Fan, M. Zhong, S. Xiao, D. Zhang, J. Yang, J. Zheng, Dual-stimulus bilayer hydrogel actuators with rapid, reversible, bidirectional bending behaviors, J. Chem. Mater. C 7(17) (2019) 4970-4980.

[29] L. Liu, S. Jiang, Y. Sun, S. Agarwal, Giving direction to motion and surface with ultra-fast speed using oriented hydrogel fibers, Adv. Funct. Mater. 26(7) (2016) 1021-1027.

[30] M. Zhou, J. Gong, J. Ma, Continuous fabrication of near-infrared light responsive bilayer hydrogel fibers based on microfluidic spinning, e-Polymers 19(1) (2019) 215-224.

[31] W. Razzaq, C.A. Serra, L. Jacomine, D. Chan-Seng, Microfluidic elaboration of polymer microfibers from miscible phases: Effect of operating and material parameters on fiber diameter, J. Taiwan Inst. Chem. Eng. 132 (2022) 104215.

[32] W. Razzaq, C.A. Serra, D. Chan-Seng, Production of Janus/Hecate microfibers by microfluidic photopolymerization and evaluation of their potential in dyes removal, Chem. Commun. 58 (2022) 4619-4622.

[33] P.J. Roth, M. Collin, C. Boyer, Advancing the boundary of insolubility of non-linear PEG-analogues in alcohols: UCST transitions in ethanol–water mixtures, Soft Matter 9(6) (2013) 1825-1834.

[34] K.F. Mueller, Thermotropic aqueous gels and solutions of *N*,*N*-dimethylacrylamide-acrylate copolymers, Polymer 33(16) (1992) 3470-3476.

[35] S. Saeki, N. Kuwahara, M. Nakata, M. Kaneko, Upper and lower critical solution temperatures in poly (ethylene glycol) solutions, Polymer 17(8) (1976) 685-689.

[36] B. Hammouda, D. Ho, S. Kline, SANS from poly(ethylene oxide)/water systems, Macromolecules 35(22) (2002) 8578-8585.

[37] S. Sun, P. Wu, On the thermally reversible dynamic hydration behavior of oligo(ethylene glycol) methacrylate-based polymers in water, Macromolecules 46(1) (2013) 236-246.

[38] B. Peng, N. Grishkewich, Z. Yao, X. Han, H. Liu, K.C. Tam, Self-assembly behavior of thermoresponsive oligo(ethylene glycol) methacrylates random copolymer, ACS Macro Lett. 1(5) (2012) 632-635.

[39] F. Käfer, F. Liu, U. Stahlschmidt, V. Jérôme, R. Freitag, M. Karg, S. Agarwal, LCST and UCST in one: Double thermoresponsive behavior of block copolymers of poly(ethylene glycol) and poly(acrylamide-*co*-acrylonitrile), Langmuir 31(32) (2015) 8940-8946.

[40] H.-Y. Tian, J.-J. Yan, D. Wang, C. Gu, Y.-Z. You, X.-S. Chen, Synthesis of thermo-responsive polymers with both tunable UCST and LCST, Macromol. Rapid Commun. 32(8) (2011) 660-664.

[41] Á. Szabó, G. Bencskó, G. Szarka, B. Iván, Thermoresponsive UCST-type behavior of interpolymer complexes of poly(ethylene glycol) and poly(poly(ethylene glycol) methacrylate) brushes with poly(acrylic acid) in isopropanol, Macromol. Chem. Phys. 218(5) (2017) 1600466.

[42] Z. Osváth, B. Iván, The dependence of the cloud point, clearing point, and hysteresis of poly(*N*-isopropylacrylamide) on experimental conditions: The need for standardization of thermoresponsive transition determinations, Macromol. Chem. Phys. 218(4) (2017) 1600470.

[43] M. Xia, Y. Cheng, Z. Meng, X. Jiang, Z. Chen, P. Theato, M. Zhu, A novel nanocomposite hydrogel with precisely tunable UCST and LCST, Macromol. Rapid Commun. 36(5) (2015) 477-482.

[44] G. Zhang, J. Lei, L. Wu, C. Guo, J. Fang, R. Bai, I. Wyman, Poly(imidazoled glycidyl methacrylate-*co*-diethyleneglycol methyl ether methacrylate) – A new copolymer with tunable LCST and UCST behavior in water, Polymer 157 (2018) 79-86.

[45] C. Nam, J. Yoon, S.A. Ryu, C.H. Choi, H. Lee, Water and oil insoluble PEGDA-based microcapsule: Biocompatible and multicomponent encapsulation, ACS Appl. Mater. Interfaces 10(47) (2018) 40366-40371.

[46] C.A. Warr, H.S. Hinnen, S. Avery, R.J. Cate, G.P. Nordin, W.G. Pitt, 3D-Printed microfluidic droplet generator with hydrophilic and hydrophobic polymers, Micromachines 12(1) (2021) 91.